Automating Multiple-Throw Multilateral Surgical Suturing with a Mechanical Needle Guide and Sequential Convex Optimization

Siddarth Sen*[1], Animesh Garg*[2], David V. Gealy[3], Stephen McKinley[3], Yiming Jen[1], Ken Goldberg[2]

***Abstract*— Suturing is a ubiquitous sub-task in surgery. To explore supervised automation of multi-throw suturing in Robot-Assisted Minimally Invasive Surgery, we present a novel mechanical needle guide design and an optimization framework to optimize needle size, needle trajectory and control parameters for two arms using sequential convex programming. We also develop a model-based needle tracking system to achieve closed loop control. We show that in comparison with the standard 8mm needle driver, our Jaw-mounted Needle Guide (JNG) improves accuracy of needle orientation by 3x on average in the presence of needle orientation noise of up to 30° in either axis, and reduces the need for needle re-alignment before subsequent needle insertion. Use of real-time needle tracking can estimate pose with a standard deviation of 2.94 mm and 6.8°. We demonstrate our framework on a 4-throw suturing task on a da Vinci Research Kit using tissue phantoms for skin and subcutaneous fat. We evaluate suturing performance based on success rate and compare completion time with suturing demonstrations in JIGSAWS dataset [5]. We evaluate effects of pose constraints on the suture path with respect to path length and tissue trauma. Our results indicate that dVRK can perform 4-throw suturing at $\approx 1/3$rd of human speed at a success rate of 50% for the 4-throw task, successfully completing 86% suture throws attempted. Task videos and data available at: berkeleyautomation.github.io/amts**

I. Introduction

Robotic Surgical Assistants (RSA) have facilitated the pairing of human surgical expertise with the precision and repeatability of robots in minimally invasive surgery. Intuitive Surgical's da Vinci System, facilitated over 570,000 procedures worldwide in 2014 with 3000 systems [8]. RSAs are currently controlled by surgeons using pure tele-operation. Automation of tedious and frequent surgical sub-tasks such as suturing has the potential to reduce surgeon tedium and fatigue, operating time, and enable supervised tele-surgery.

We consider automation of multi-throw suturing (MTS). MTS under tele-operation remains a tedious and time consuming task with sequential sutures without knot tying. MTS is beneficial for minimizing wound tension; it is frequently used in surgery for external tissues such as facial and abdominal [6], as well as for internal tissues such as intestinal anastomosis [1]. Automation in suturing has been widely explored, with studies addressing individual challenges in (a) interaction with deformable tissue [9, 10], (b) multilateral manipulation of needle and suture [35], and (c) hierarchical models for multi-step task planning [12].

* These authors contributed equally to the paper
The authors are with University of California, Berkeley CA USA
[1]EECS, {siddarthsen, yjen}@berkeley.edu
[2]IEOR & EECS, {animesh.garg, goldberg}@berkeley.edu
[3]Mechanical Engineering, {dgealy, mckinley}@berkeley.edu

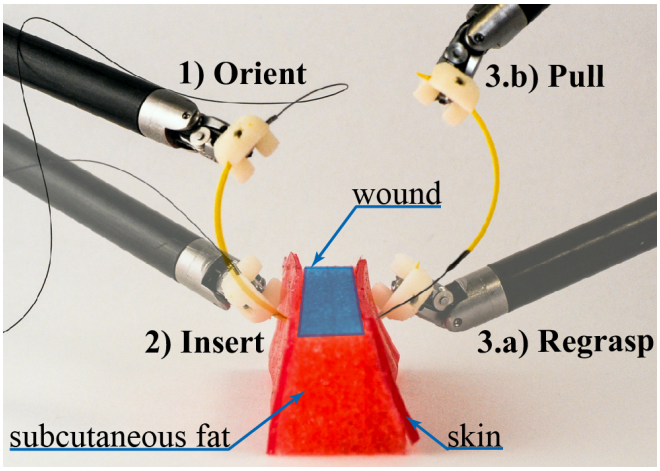

Fig. 1: Each suturing throw consists of four steps: (1) Needle Orientation (2) Needle Push, (3.a) Needle Grasp, and (3.b) Suture Pull shown here in time-lapse view with two da Vinci Needle Driver tools. Step (4) Needle hand-off after the suture pull is not shown here (see Sec.VI). It also shows the experimental suturing setup with tissue phantom that mimics two layers of skin surrounding subcutaneous fat.

We present preliminary results in automation of multi-throw suturing (MTS). We propose a framework of software and hardware that enables robust autonomy in MTS and perform time comparisons with manually tele-operated demonstrations. This paper builds upon prior art in optimization based planning [4, 28], sub-task level segmentation of demonstrations [16, 17], gripper mounted interchangeable tools [20] and building & tuning finite state machines [22]. We propose a segmentation of the single throw suture (STS) into 4 steps: (1) Needle Orientation, (2) Needle Insertion, (3) Needle Re-grasp and Pull and (4) Needle Hand-Off as illustrate in Figure 1. The MTS finite state machine uses needle pose manipulation and estimation to transition between states.

Contributions: (1) We address the uncertainty in the the Needle Re-grasp and Needle Hand-Off with a novel mechanical design of a gripper Jaw-mounted Needle Guide (JNG) that passively re-orients the needle into a known position upon gripper closure. (2) We formulate the Needle Insertion problem as a non-convex curvature-constrained motion planning problem. (3) We also develop a real time model based needle tracking algorithm to complement the JNG.

We find that JNG improves repeatability by 10**x** and orientation accuracy by 3**x** as compared with standard 8mm needle driver. We demonstrate our approach on a subtask

Preprint submitted to 2016 IEEE International Conference on Robotics and Automation. Received September 15, 2015.

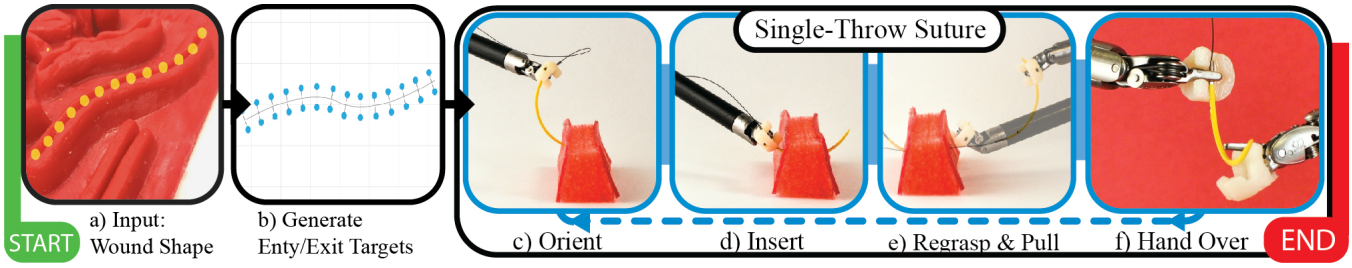

Fig. 2: The Multi-Throw Suturing Finite State Machine. First the surgeon specifies a wound shape along with wound width & depth and suture pitch. Then the system computes entry and exit points, and generates optimized trajectory and needle size for every suture throw. Then Single-throw Suture steps (c)-(f) are repeated with visual feedback for each suture throw until completion.

from the Fundamental Skills of Robotic Surgery [36] – 4-throw suturing task. In our physical experiments, we achieved a success rate of 50% for the 4-throw task and 86% of attempted suture throws were completed. The system is currently 3**x** slower than human surgeons [5].

II. Related Work

RSAs are increasingly being used in a variety of surgical interventions such as such as prostectomy, uterectomy, and tumorectomy within the abdominal and thoracic cavities [2, 26]. Moustris et al. [21] and Kranzfelder et al. [15] have reviewed recent developments in semi-autonomous and autonomous execution of various surgical procedures such as tumor ablation [7] and multilateral tumor debridement [14].

The *Fundamental Skills of Robotic Surgery* (FSRS) is a representative set of frequently occurring procedures in surgery, used for surgical training and evaluation [36]. Multi-throw suturing (MTS) is also one of the tasks recommended by FSRS. Prior work in surgical automation has modeled the basis set of surgical motions as "Language of Surgery" with surgemes (Hager et al.) [30]. Many of the FSRS procedures, including MTS, are decomposable into long sequences of simpler sub-tasks. This decomposition allows parameterizing and constructing Finite State Machines (FSM) for complex procedures such as MTS.

Automation in the surgical domain has explored building these FSMs for a variety of procedures such as multilateral tissue debridement [14], multilateral pattern cutting [22] and multi-step procedures such as tumor localization and resection [20]. It has been shown that FSMs can be built with a learning by observation approach for robust automation in surgical sub-tasks involving cutting by provisioning for failure recovery behavior [20, 22]. Our recent results on segmentation of multi-step task demonstrations [16] show that unsupervised recovery of semantic transitions is feasible and can be analyzed to construct FSMs for these multi-step procedures. At the same time, recent works have also explored the use of learning techniques to infer surgeme transitions from demonstration data [17, 25].

Automation of Suturing: Suturing automation has been widely explored in research given the importance and frequency of this subtask. Starting in early 2000s, Kang et al. [12] devised a specialized stitching device which is capable of creating a knot. Mayer et al. used a recurrent neural net as part of a controller to learn knot tying with three industrial arms using motion primitives from human demonstrations[19]. Van den Berg et al. used iterative learning control to extract smooth trajectories for performing knot tying at super-human speeds [37]. More recently, Schulman et al. used a learning by demonstration approach to warp recorded expert demonstrations and perform suturing in simulation[32]. Padoy et al. showed execution of a human-robot collaborative suturing, but the sections requiring interactions such as needle insertion and hand-off were manual [27]. [35] automated of tissue piercing with needle but did not complete autonomous MTS.

Suture Path Planning: A number of preceding studies use a fixed curvature needle path. However, needles might not always follow their natural curvature. Interaction with tissue may deflect the needle and if the end point pose constraints necessitate non-orthogonal exit. Jackson et al. [10] used a reference trajectory to create an analytical solution allowing for needle insertion without considering uncertainty or robot pose constraints. However, using optimization based planning allows for extensions that address these limitations. Recent results in motion planning have shown that Sequential Convex Programming (SCP) based planning, such as [31] can be better than sampling based planners. Hence, we choose to formulate suture planning as a curvature constrained SCP based optimization problem solved with custom implementation.

Needle Orientation Uncertainty: Suturing success is dependent on planning complex needle motions, needle handling dexterity, and maintaining correct needle orientation during the needle insertion in tissue. Incorrect placement of the needle in the gripper may result in a bent needle, difficult skin penetration, or an undesirable tissue entry angle. However, maintaining and estimating needle orientation is a challenge without accurate needle tracking. Authors of [10] also note that a system for MTS would need both planning and visual feedback. There have been studies focusing on needle tracking within surgical settings as shown in [11, 24, 34].

Medical device manufacturers have explored the use of self-righting needle holders for manually held laparoscopic tools [18, 29]. However, these instruments have not been used for automated control and are not available for robotic MIS systems.

There are un-modeled uncertainties in gripper-needle and needle-tissue interactions that can cause the needle to drift from an original plan. While others have studied aspects

Preprint submitted to 2016 IEEE International Conference on Robotics and Automation. Received September 15, 2015.

of the problem: planning, needle tracking, and instrument design; We are not aware of any system that can perform autonomous multi-throw suture reliably.

III. Problem: Formulation and Definitions

Surgeons follow suturing task guidelines such as: entering the tissue orthogonally, minimizing tissue-needle wrench, choosing a correct needle size for adequate suture depth, and sufficient length of needle protrusion to enable pulling the needle out of the other end. While a needle would follow a constant curvature path through rigid objects, tissue is deformable. Thus we model the needle path to allow bounded rotations about the needle tip while the needle is inserted. However, needle paths that do not follow the natural curvature of the needle can result in tissue damage, hence we define a bounded deviation (γ) from needle curvature, κ, that can be visualized as a cone at each point as illustrated in Figure 4. Further we monotonically reduce γ as the needle progresses to minimize tissue damage. Furthermore, the success of suturing is highly sensitive to needle pose uncertainty at entry point, and the effect this uncertainty is illustrated in Figure 3.

Assumptions: We assume that tissue is homogeneous and deformable. Since real tissues have very high variability in stiffness and homogeneity, we do not model interactions between tissue and needle either via simulation or explicit spring mass system modeling. We assume that the needle is rigidly held in the gripper and can only move forward in the tangential direction of the tip. However, bounded reorientation of the needle tip is permitted as it is inserted through tissue. We assume that our system has access to a continuous range of needle sizes. Needle vary in lengths(in increments of 1mm), diameter and curvature ($\{\frac{3}{8}, \frac{1}{2}$, or $\frac{5}{8}\}$).

Input: The wound shape is provided as input with the points $\mathcal{M} = [M_1, M_2, \ldots, M_D] \in \mathbb{R}^3$ representing the spline of wound surface. Also input is suture depth d, suture width l, and a pair of entry/exit poses ($P_i, P_f \in SE(3)$) as illustrated in Figure 3. Further, we are also given suture pitch w – distance between consecutive throws of suture.

Output: The system needs to find a set of suture throws $\mathcal{S}$, where $\forall\, S_j \in \mathcal{S}$, calculate an optimized sequence of needle tip poses $\mathcal{X}_j \in SE(3)$ satisfying the the suture depth and suture width constraints or report that no such path plan exists. The system also needs to choose a needle diameter and length.

The entry and exit positions at each suture S_j are linearly interpolated using P_i, P_f keeping the orientation constant. Further, since the transform from gripper to needle is calculated through needle tracking T_G^N, the control input is then a linearly transformed sequence of needle tip poses $X_t^g = T_G^N X_t, \forall t \in T$.

A. Curvature Constrained Kinematic Model:

The needle trajectory is discretized into time intervals $\mathcal{T} = \{0, 1, \ldots, T\}$, where the needle moves a fixed amount (Δ) in each time step. At each time step the needle's pose is parametrized as $X_t \in SE(3)$.

We model our trajectory to be composed of $T-1$ circular arcs with curvature κ_t between every consecutive pair of needle poses (X_t, X_{t+1}). We model our control of the needle at each time step as a rotation and insertion where at each time step the pose X_t is propagated a distance Δ to X_{t+1}. Although a needle naturally follows a path of constant curvature, the needle tip can be reoriented at each time step to change the local curvature by $\bar{\gamma}_t$. Thus at each time step the path curvature κ_t can be expressed as $\kappa_t = \kappa + \bar{\gamma}_t$ where κ is the curvature of the needle and $\bar{\gamma}_t$ is the change in curvature applied at each time step. Poses between consecutive time steps can then be related as:

$$X_{t+1} = \exp(u_t^{\wedge}) \cdot X_t \tag{1}$$

where $u_t = \begin{bmatrix} 0 & 0 & \Delta & \Delta\kappa_t & 0 & 0 \end{bmatrix}^T$.

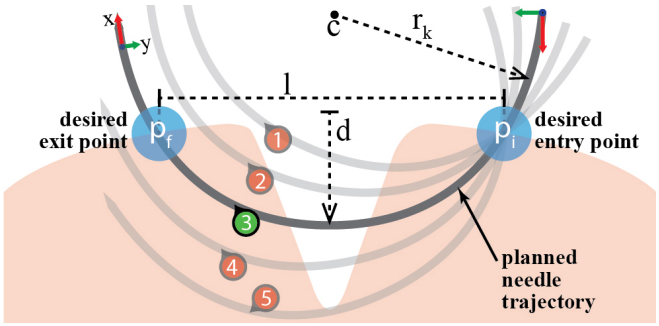

Fig. 3: Needle trajectory labeled (3) shows the desired trajectory along with poses at entry and exit points from the tissue. The success of suturing depends on correct orientation of needle with respect to the tissue. For example, uncertainty in needle pose at entry point may result in the needle not connecting opposite tissue sides (1), not making sufficiently deep insertion to hold the suture securely (2), not having enough length of needle at the other end to enable re-grasping (4), or passing completely under the wound & not coming out of tissue at all (5).

B. Evaluation Metric:

Since minimizing trauma is one of the main factors in suturing, we consider two criteria: Trajectory Length (TL) and Swept Needle Volume (SNV). We assume that SNV is linearly proportional to volume swept by needle due to rotations at the tip. We define TL: $\mathcal{C}. = T\Delta$ in eq(2), and SNV: $\sum_t \gamma_t t \Delta$. We also measure the performance of the closed loop 4-throw suturing on: task completion time, and errors modes.

IV. Suture Path Planning

The Suture Path Planning (SPP) problem can be formulated as a non-convex curvature constrained motion planning problem solved with a series of locally convex approximations using sequential convex programming(SCP).

The needle trajectory is discretized into time intervals $\mathcal{T} = \{0, 1, \ldots, T\}$, where the needle moves a fixed amount (Δ) in each time step. At each time step the needle's pose is parametrized as $X_t \in SE(3)$.

Optimization Model:

For notational convenience we concatenate the states from all time steps as $\mathcal{X} = \{X_t : t \in \mathcal{T}\}$ and control variables as $\mathcal{U} = \{\kappa, \Delta, \gamma_t : t \in \mathcal{T}\}$

Preprint submitted to 2016 IEEE International Conference on Robotics and Automation. Received September 15, 2015.

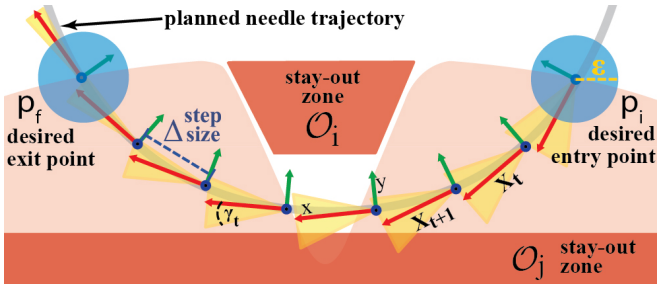

Fig. 4: The optimization steps and non-holonomic motion at each time-step. The figure shows stay-out zones $\mathcal{O}_i$, trajectory poses X_t, step-size Δ, needle radius r, and γ-cone of allowed rotation at each X_t.

$$SPP: \underset{\mathcal{X},\mathcal{U}}{\text{minimize}} \quad \alpha_\Delta C_\Delta + \alpha_I C_I \tag{2}$$

$$\text{s.t.} \quad \log(X_{t+1}\cdot(\exp(u_t)\cdot X_t)^{-1})^\vee = 0_6 \tag{3}$$

$$|\bar{\gamma}_t| \le \gamma_t \qquad \forall t \tag{4}$$

$$T\Delta + 2l_g - \frac{2\pi l_n}{\kappa} \le 0 \tag{5}$$

$$\text{sd}(X_t, \mathcal{O}_i) \ge d_s, \qquad \forall i \tag{6}$$

$$X_0 \in \mathcal{B}(p_i,\varepsilon),\ X_T \in \mathcal{B}(p_f,\varepsilon) \tag{7}$$

Each term in the above formulation is described below:

Costs (Eq. (1)): We assume the volume of needle in tissue is proportional to tissue trauma and hence we penalize longer trajectories such that $C_\Delta = T\Delta$. Furthermore, surgical guidelines suggest that the needle entry pose should be orthogonal to the tissue surface. The weights α_Δ and α_I are hyper-parameters that are tuned in the optimization.

Kinematic Constraints (Eq. (3)): The kinematic constraint in Eq.1 can be transformed using the exponential log map into the standard equality constraint in Eq. 3. In Eq.4 we bound the magnitude of $\bar{\gamma}_t$ to minimize tissue damage. We select γ_t to be monotonically decreasing with t because needle rotations away from its natural curvature cause greater damage the further the needle is inserted into tissue.

Needle Length Constraints (Eq. (5)): The length of the insertion trajectory is constrained to be less than the length of needle and should allow for grippers to hold the needle on both end. Let $l_n = \frac{5}{8}$, then based on our problem formulation, the length of the longest needle with a given curvature κ is $\frac{2\pi l_n}{\kappa}$. Le l_g be the length of needle occupied by a gripper when it is holding a needle. Then sum of the trajectory length plus $2l_g$ should be less than the length of the needle. This inequality is reformulated in standard form in Eq. 5.

Collision Constraints (Eq. (6)): We impose constraints to ensure that our trajectory avoids collisions with pre-defined stay out zones. The stay out zones can be non-convex meshes that can be decomposed into convex sub meshes [3], $\mathcal{O} = \{\mathcal{O}_1, \ldots, \mathcal{O}_i\}$. The stay out mesh can also be artificially constructed from the desired suture depth. We ensure that the signed distance between each X_{t+1} and each convex mesh in $\mathcal{O}$ is greater than a safety margin hyperparameter d_s.

Entry and Exit Point Constraints (Eq. (7)): We constrain the start and end poses of the trajectory to be within an ε-Ball of the calculated entry(p_i) and exit(p_f) poses. This can be expressed as $\log(p_i \cdot X_0^{-1})^\vee \le \varepsilon \cdot \mathbf{1}_6$ for the start pose of the trajectory. The end pose constraint follows a symmetric formulation.

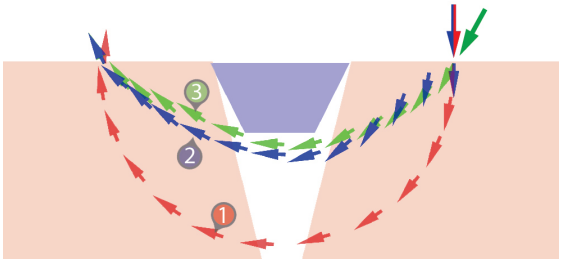

Fig. 5: The side view of three needle trajectories generated by SPP. Trajectory 1 and 3 are constant curvature trajectories whereas trajectory 2 is a variable curvature trajectory.

We note that a single value of Δ is chosen for all time steps instead of having a different Δ_t for each time. as the latter is experimentally found to disagree numerically with the findings of Duan et al. [4].

Trajectory Optimization

Sequential convex programming is a general approach for solving constrained, non-convex optimization problems.The use of SCP based motion planning algorithm is described in full detail in [33]. The optimization problem outlined in Eq. (2) is, however, described directly over the set of poses X. Optimizing directly over these poses can lead to poor results due the the number large number of free variables in the rotation matrix of each pose.

Figure 5 shows the SPP output for three different sets of pose constraints. For #1, we restrict rotation about needle tip ($\gamma_t = 0, \forall t$). Coupled with the orthogonality constraint at entry/exit, this results in a constant curvature path along the needle radius. For #3, we relax the pose constraints, resulting in shortest path trajectory, but with oblique entry angles. Finally for #2, similar to surgeon best practices, orthogonality is enforced only at entry pose, and γ_t is set to a monotonically decreasing sequence in t. It results in rotations about needle tip, to achieve an assymmetric trajectory satisfying pose constraint at entry. Comparing the lengths normalized to the longest trajectory (#1), we find that trajectories #2 and #3 have 0.72 and 0.70 lengths, while #2 also has a SNV of 0.242.

V. Reducing Needle Pose Uncertainty

As stated in Section III and Figure 3, tissue damage is minimized with an orthogonal entry as well tangential movement of the needle tip through tissue. These guidelines require both accurate needle pose estimates at the needle entry point, as well as maintaining the needle pose with respect to the needle driver during needle manipulation.

A. Jaw-mounted Needle Guide (JNG)

Commercially available RMIS needle drivers allow handling of a variety of needle sizes, however an analysis of suturing trials in JIGSAWS dataset [5] reveals that multiple-pairs of hand-offs are required for correct needle orientation.This is because the needle held within the needle driver

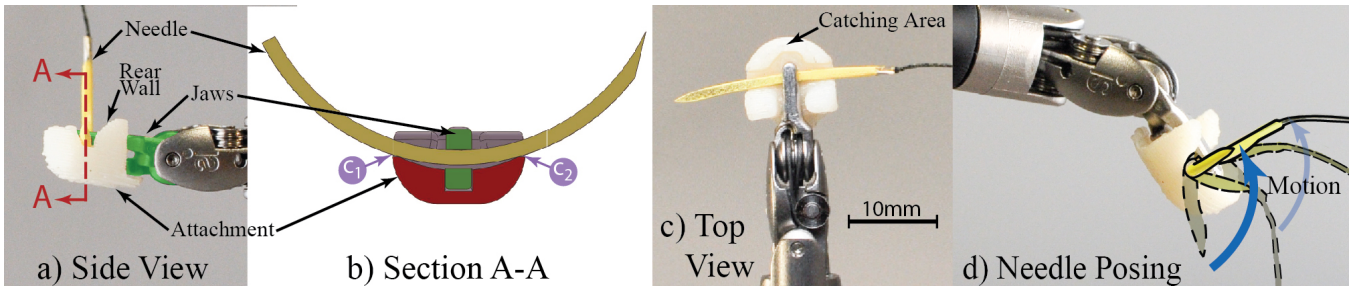

Fig. 6: This figure illustrates the design and function of the Jaw-mounted Needle Guide (JNG) made from 3D Printing. Figures (a) and (b) show a convex depression in which needle rests upon gripper closure. Figure (d) shows a time-lapse figure of the gripper closing action on needle orientation.

jaws is not fully constrained. The flat gripper surface allows rotation, and translation along the length of the needle, which can be hard to control without haptic or visual feedback.

There have been some commercial efforts to mitigate back-and forth hand-offs and uncertainty in laparoscopic surgery through passively orienting the needle on gripper closure using a '*self-righting*' gripper jaw design [18, 29]. However, these are not designed for automation, and require a complete tool-redesign.

Building upon existing work, we develop a design for a low-cost Jaw-mounted Needle Guide (JNG), for dVRK Classic 8mm Needle Driver with 6mm jaws, which works to guide and passively orient a curved needle into a stable pose upon closure of gripper jaws as illustrated in Figure 6(d). JNG reduces needle pose uncertainty in two rotational axes as shown in Section VII. This allows for a higher tolerances during needle hand-off, and hence relaxing accuracy requirements of needle tracking.

Mode of Operation: JNG is mounted axially on one of the needle driver jaws. It is designed to guide the needle towards a groove running perpendicular to the length of the gripper jaws Figure 6(b), (c). Upon closing the jaws, the needle rolls to a stable pose passing through contact points C_1 and C_2 as shown in the section view in Figure 6(b).

The size of the needle gripper is parametrized by the distance between contact points C_1, C_2 which is dependent on the curvature of the needle – a needle with a larger radius needs a wider contact grasp to enable the needle rolling upon jaw closure. As illustrated in the Figure 6(a), JNO has a rear-wall that allows the gripper to overshoot into during the pre-grasp approach. It also has a needle *catching area* in the front (Figure 6(c)) that guides the needle in the groove compensating for undershoot during pre-grasp. Both these features increasing robustness of needle manipulation.

The JNG is fabricated from ABS plastic using a Stratysys uPrint 3D printer. For an 8mm classic needle driver, using a $\frac{3}{8}$ circumference, 39mm length needle, we designed the JNG with $C_1 - C_2$ span of 10mm. Through experimental evaluation, we improved upon the JNG design to include a larger rear wall. This enabled a wider jaw opening during approach allowing for larger tolerance in needle pose uncertainty.

B. Real Time Needle Tracking

We have developed a real-time needle tracking system to provide closed loop feedback during the suturing process as summarised in Figure 7. Due to tissue and tool specularity, perception using RGBD sensing is not feasible. Our system provides 3D needle pose estimates using a custom built stereo camera pair, composed of two Prosilica GigE GC1290C cameras with 6 mm focal length lenses. The needle tracking algorithm is implemented as a ROS node that publishes real time estimates of the needle's pose. The tracking system works with partial occlusion –such as needle inside tissue or behind robot arms.

We use a model based tracking system leveraging the needle shape and color. First step in the process is *Needle Segmentation*. We use a yellow painted needle to assist in foreground-background separation. We use HSV (Hue, Saturation, Value) separation to identify needle in a cluttered environment with the open-source OpenCV library and create a set of image plane points $\mathcal{P}_I$.

Then, we leverage the circular shape of the surgical needles and their elliptical projection. We create a small set of parametrically sampled points along the length of needle model $\mathcal{P}_M$, $|\mathcal{P}_M| = 12$, and then use affine point set registration to fit the $\mathcal{P}_I$ to $\mathcal{P}_M$. Using a point set matching as a non-linear registration problem allows robustness to outliers, missing data due to occlusions, and noisy data from incorrect segmentation masks. We use the Matlab library CPD2 for solving the registration problem [23].

Using the ellipse fits on the image pair, we generate a dense set of corresponding points along the needle. This creates a robust disparity map of 3D points on the needle. A plane is then fit to the 3D points, giving the normal vector, while an average tangential direction is calculated using the 3 points on the end of the needle. Using the end point of the needle and these two vectors, a pose $p_n \in \mathbb{R}^6$ is generated. We use a 30 Hz Kalman filter to smooth needle tip pose estimates.

VI. Multi-Throw Suturing: System Design

We present a closed loop Finite State Machine (FSM) for multi-throw suturing with needle orientation tracking and multilateral needle hand-off as illustrated in Figure 2.

Given the registration of the tissue phantom in the camera frame, a Multi-throw Suture plan is generated. The SPP

Preprint submitted to 2016 IEEE International Conference on Robotics and Automation. Received September 15, 2015.

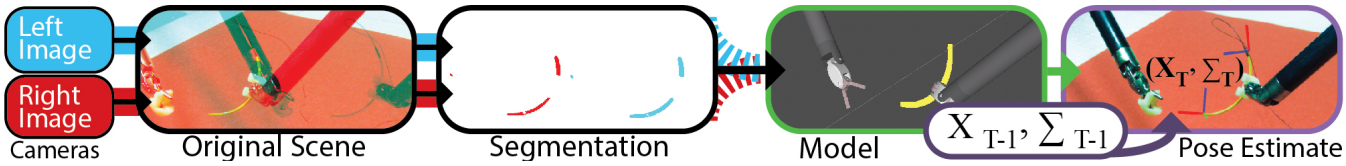

Fig. 7: This figure shows an overview of the needle tracking pipeline, from stereo images to the final needle pose estimate overlaid onto the original scene. We fuse a Kalman filter estimate with current camera estimate to compute the final estimate. The tracking system is robust to outliers and missing data in the segmentation masks.

algorithm is used to generate needle trajectories and a suggested needle curvature. Each throw in the task consists of the following sequence of sub-tasks which were segmented on the basis of manual surgeme labels for suturing in the JIGSAWS dataset:

1. Needle Orientation and 2. Insertion We note that since suture thread is not tracked, the needle ends are indistinguishable. Hence, we generate end poses for both needle ends and maintain a track of both the front and rear ends. Let the two ends of the needle be the tip N_T and the tail N_S connected to suture. Starting with the needle held in the right gripper at N_S, the system creates an initial pose estimate. Using this estimate, the robot brings the needle to a pose so that the needle plane is aligned with camera's image plane, allowing for an occlusion free view of the needle. This improves the needle pose estimate, and the system executes a trajectory for the N_T using the planner described in previous sections. We note that at this point suture path can be re-planned after every user-specified rolling time horizon.

3. Needle grasp and Pull Through After the right arm guides the needle through tissue, the left arm grasps the needle at N_T and pulls it through and out of the tissue. To minimize tissue trauma, the needle is pulled tangentially to the needle tip minimizing translational motion within the tissue, by rotating about the center of curvature of the needle. Once the needle is completely outside the tissue, it is pulled away sufficiently to tighten the tissue. The system decides how far to pull the needle away based on how much slack is available in the suture thread. The system estimates the amount of slack lost in the suture thread after each throw by modeling the length of thread between consecutive entry points as a helical loop with radius equal to the radius of the needle and pitch equal to the suture pitch. This provides a conservative estimate of how much slack is lost in each throw and the system decreases the distance it pulls the thread away by this amount after each throw.

4. Needle Hand-Off Our needle tracking algorithm estimates the pose of the needle end N_S while it is grasped at N_S. Similar to step (1), to improve needle pose estimates the left arm aligns the needle in the image plane to provide an un-occluded view. Now, using the estimated pose of N_S, the left arm moves to allow the right arm to grasp N_S in a pose necessary for the next needle insertion step.

We note that since there may be inherent pose errors in camera-robot registration and robot kinematics, the hand-off process is performed by simultaneously engaging the right arm at N_S while disengaging the left arm at N_T. A slight error in coordination will result in failed transfer due to stresses generated in the needle. Use of the Needle Guides on both gripper ends facilitates this process because the grooves provide a space resulting in a partial cage instead of a force closure during the hand-off.

VII. Experimental Evaluation

A. dVRK: Hardware and Software

We use the Intuitive Surgical da Vinci Research Kit (dVRK) surgical robot assistant as in [22], along with open-source electronics and software developed by WPI and Johns Hopkins University [13]. We use a pair of 8mm Needle Drivers with each gripper having one Jaw-mounted Needle Guide (JNG). The software system is integrated with ROS and allows direct robot pose space control, working in Cartesian space instead of commanding motor torques.

B. Experimental Evaluation of Needle Tracking

The size and shape of needles makes it difficult to obtain ground truth pose estimates using techniques like fiducial-based motion capture. Instead we designed an experiment to indirectly verify the efficacy of our needle tracking system. The robot holds the needle rigidly in its gripper and moves the needle to random positions in the workspace. Note that the relative pose of the needle with respect to the gripper position never changes. At each random position the robot pauses and uses the needle tracking system to compute the needle's relative pose with respect to the gripper pose (estimated from kinematics). Poses at 20 different random locations were recorded. The following vector shows the standard deviation in x,y,z in mm and in roll, pitch, and yaw in degress respectively in the needle's relative pose: $[2.18, 1.23, 1.54, 2.495, 4.699, 4.329]$. The low error in every dimension suggests that our estimates of the needle's relative pose are nearly identical at each random location. This matches up with the ground truth that the needle's relative pose never changes. The errors reported are not just the error produce by the needle tracker but the composite error produced from needle tracking, camera-robot registration, and robot kinematics. However it provides an upper bound on the needle tracking error and is representative of error that our system must be robust to.

C. Evaluation of Jaw-mounted Needle Guide (JNG)

1. Stationary Needle Pick up: In this experiment we evaluate the Jaw-mounted Needle Guide. For each trial, the needle is placed in the same location and the robot is given a grasp pose to pick it up. After the needle is picked up, the robot brings the needle to a known location and the needle's pose is recorded using our needle tracker. We repeat this process over ten trials. Due to noise in the robot's kinematics and needle's starting pose, the needle is grasped slightly

TABLE I: Needle Guide Evaluation: Stationary Pick up

Stationary Grasp Orientation		**Error**					
	Succ. Grasps	x (mm)	y (mm)	z (mm)	yaw (deg)	pitch (deg)	roll (deg)
Without JMG	100%	2.511	1.434	4.838	20.547	7.584	6.472
With JMG	100%	0.199	0.158	0.177	0.926	1.094	0.664
Perturbed Grasp Orientation		**Error**					
	Successful Grasps	x (mm)	y (mm)	z (mm)	yaw (deg)	pitch (deg)	roll (deg)
Without JMG	100%	2.01	2.59	5.95	15.54	12.74	7.62
With JMG	91.66%	1.58	1.15	1.19	5.55	3.97	6.34

differently each time, resulting in variances in the needle's pose.

In the second part of the experiment we perturb the orientation of the robot's grasp pose to evaluate robustness to uncertainty in orientation. The grasp pose is perturbed from -30 degrees to 30 degrees in yaw, pitch, and roll. Our results show that the use of JNGs results in a 3x reduction in needle pose uncertainty over standard Needle Driver.

D. Robot Experiments: Four Throw Task

We used a suturing phantom made with foam to mimic subcutaneous fat tissue with a layer of 1mm thick skin using (shore hardness 2A) *DragonSkin 10 Medium* Silicone Rubber (*Smooth-On*).

In this experiment, the system tries to complete a closed loop four throw suturing task. We provided the system entry and exit poses on opposite surfaces of the tissue phantom as well as a desired suture depth. Based on the output needle curvature, we selected a 39mm long, $3/8$ reverse cutting needle to perform the suturing throws. For each trial we record time to completion as well as the failure mode if necessary. The robot moves at a top speed of 3cm/s.

VIII. Conclusion and Future Work

Initial experiments suggest the multi-throw suturing (MTS) can be automated using the proposed framework but performance times are only 30% that of human teleoperation. Our system uses are larger workspace and also pauses 8s per suture throw to align the needle for improvement in pose prediction. We will explore avenues of relaxing this requirement, and using higher speeds to improve task completions times.

Further our observations suggest that the use of Jaw-mounted Needle Gripper(JNG) along with Needle Tracking substantially improves needle orientations and hence enable the MTS task. The next steps are to evaluate the use of swept needle volume as objective cost and explore augmenting the needle state with needle pose belief for uncertainty compensation through optimization re-planning. Finally we will explore the modification of JNG to enable knot tying.

TABLE II: This table compares the performance of our autonomous suturing system with different skill levels of surgeons in the JIGSAWS data-set[5]

Operator Mode	Average Time for 1-Throw (s)	Average time for 4-throw Task (s)
Expert	19.03	87.02
Intermediate	18.57	87.89
Novice	32.14	136.85
Autonomous (Our Approach)	112.33	383.00

TABLE III: Results for 4 Throw Suturing. 14 trials were performed, with a 50% success rate. For failed states, "N.I" represents incorrect needle orientation or insertion, "G.P." represents incorrect needle re-grasp and pull after insertion, and "H.O" represents failure in needle hand-off respectively. The test setup was varied with translation of simulated wound along the wound axis.

Trial	4-Throw Success	# of Throws Completed (Attempted)	Failure Mode	Trans. in X	Suture Pitch	Total Time(s)
1	Failure	1 (2)	G.P.	-3mm	3mm	-
2	Failure	2 (3)	G.P.	-3mm	3mm	-
3	Failure	3 (4)	G.P.	-2mm	3mm	-
4	Success	4 (4)		-1mm	3mm	387
5	Success	4 (4)		0mm	3mm	380
6	Success	4 (4)		0mm	3mm	380
7	Success	4 (4)		0mm	3mm	383
8	Failure	2 (3)	H.O.	1mm	3mm	-
9	Failure	2 (3)	N.I.	1mm	3mm	-
10	Failure	3 (4)	G.P.	2mm	3mm	-
11	Success	4 (4)		3mm	3mm	393
12	Success	4 (4)		4mm	3mm	383
13	Success	4 (4)		5mm	3mm	382
14	Failure	3 (4)	G.P.	6mm	3mm	-
Mean	50%	3.14				384
Std Dev		1.027		Single Throw Success Rate: 86.3%		

Acknowledgements This work is supported in part by a seed grant from the UC Berkeley Center for Information Technology in the Interest of Science (CITRIS), and by the U.S. National Science Foundation under Award IIS-1227536: Multilateral Manipulation by Human-Robot Collaborative Systems. We thank Intuitive Surgical, Simon DiMao, and the dVRK community for support; NVIDIA for computing equipment grants; Andy Chou and Susan Lim for developmental grants; and Dr. Walter Doug Boyd for insights on suturing; Jeff Mahler, Sanjay Krishnan and Florian Pokorny for reviewing drafts.

References

[1] J. M. Burch, R. J. Franciose, E. E. Moore, W. L. Biffl, and P. J. Offner, "Single-layer continuous versus two-layer interrupted intestinal anastomosis: a prospective randomized trial," *Annals of surgery*, 2000.

[2] A. Darzi and Y. Munz, "The impact of minimally invasive surgical techniques," *Annu. Rev. Med.*, 2004.

[3] F. De Goes, S. Goldenstein, and L. Velho, "A hierarchical segmentation of articulated bodies," in *Computer Graphics Forum*, 2008.

[4] Y. Duan, S. Patil, J. Schulman, K. Goldberg, and P. Abbeel, "Planning locally optimal, curvature-constrained trajectories in 3D using sequential convex optimization," in *2014 IEEE International Conference on Robotics and Automation (ICRA)*, 2014.

[5] Y. Gao, S. Vedula, C. Reiley, N. Ahmidi, B. Varadarajan, H. Lin, L. Tao, L. Zappella, B. Bejar, D. Yuh, C. Chen, R. Vidal, S. Khudanpur, and G. Hager, "The JHU-ISI Gesture and Skill Assessment Dataset (JIGSAWS): A Surgical Activity Working Set for Human Motion Modeling," in *Medical Image Computing and Computer-Assisted Intervention (MICCAI)*, 2014.

[6] J. Hochberg, K. M. Meyer, and M. D. Marion, "Suture choice and other methods of skin closure," *Surgical Clinics of North America*, vol. 89, no. 3, pp. 627–641, 2009.

[7] D. Hu, Y. Gong, B. Hannaford, and E. J. Seibel, "Semi-autonomous Simulated Brain Tumor Ablation with RavenII Surgical Robot using Behavior Tree," in *IEEE Int. Conf. on Robotics and Automation*, 2015.

[8] Intuitive Surgical, "Annual report 2014." [Online]. Available: http://investor.intuitivesurgical.com/phoenix.zhtml?c=122359&p=irol-IRHome

[9] M. C. Jackson, Russell C.and Cavusoglu, "Modeling of needle-tissue interaction forces during surgical suturing," in *2012 IEEE International Conference on Robotics and Automation (ICRA)*, 2012.

[10] R. C. Jackson and M. C. Cavusoglu, "Needle path planning for autonomous robotic surgical suturing," in *Proc. IEEE Int. Conf. Robotics and Automation (ICRA)*, 2013.

[11] R. C. Jackson, R. Yuan, D.-L. Chow, W. Newman, and M. C. Cavusoglu, "Automatic initialization and dynamic tracking of surgical suture threads," in *IEEE Int. Conf. Robotics and Automation*, 2015.

[12] H. Kang and J. T. Wen, "Autonomous suturing using minimally invasive surgical robots," in *Control Applications, 2000. Proceedings*

of the 2000 IEEE International Conference on. IEEE, 2000, pp. 742–747.

[13] P. Kazanzides, Z. Chen, A. Deguet, G. Fischer, R. Taylor, and S. DiMaio, "An Open-Source Research Kit for the da Vinci Surgical System," in *IEEE Int. Conf. Robotics and Automation (ICRA)*, 2014.

[14] B. Kehoe, G. Kahn, J. Mahler, J.-H. Kim, A. Lee, A. Lee, K. Nakagawa, S. Patil, W. D. Boyd, P. Abbeel, and K. Goldberg, "Autonomous multilateral debridement with the Raven surgical robot," *Robotics and Automation (ICRA), 2014 IEEE International Conference on*, 2014.

[15] M. Kranzfelder, C. Staub, A. Fiolka, A. Schneider, S. Gillen, D. Wilhelm, H. Friess, A. Knoll, and H. Feussner, "Toward increased autonomy in the surgical or: needs, requests, and expectations," *Surgical endoscopy*, vol. 27, no. 5, pp. 1681–1688, 2013.

[16] S. Krishnan*, A. Garg*, S. Patil, C. Lea, G. Hager, P. Abbeel, and K. Goldberg (*denotes equal contribution), "Transition state clustering: Unsupervised surgical trajectory segmentation for robot learning," in *Int. Sym. of Robotics Research*. Springer STAR, 2015.

[17] C. Lea, G. D. Hager, and R. Vidal, "An improved model for segmentation and recognition of fine-grained activities with application to surgical training tasks," in *Applications of Computer Vision (WACV), 2015 IEEE Winter Conference on*. IEEE, 2015, pp. 1123–1129.

[18] D. Martin, J. Woodard, C. Shurtleff, and A. Yoo, "Articulating needle driver," Nov. 15 2012, US Patent App. 13/466,188.

[19] H. G. Mayer, F. J. Gomez, D. Wierstra, I. Nagy, A. Knoll, and J. Schmidhuber, "A System for Robotic Heart Surgery that Learns to Tie Knots Using Recurrent Neural Networks." *IROS*, 2006.

[20] S. McKinley, S. Sen, A. Garg, Y. Jen, D. Gealy, P. Abbeel, and K. Goldberg, "Autonomous Tumor Localization and Extraction: Palpation, Incision, Debridement and Adhesive Closure with the da Vinci Research Kit," Hamlyn Surgical Robotics Conference, London.

[21] G. Moustris, S. Hiridis, K. Deliparaschos, and K. Konstantinidis, "Evolution of Autonomous and Semi-Autonomous Robotic Surgical Systems: A Review of the Literature," *Int. Journal of Medical Robotics and Computer Assisted Surgery*, vol. 7, no. 4, pp. 375–392, 2011.

[22] A. Murali*, S. Sen*, B. Kehoe, A. Garg, S. Patil, W. D. Boyd, S. Lim, P. Abbeel, and K. Goldberg, "Learning by Observation for Surgical Subtasks: Multilateral Cutting of 3D Viscoelastic and 2D Orthotropic Tissue Phantoms," in *IEEE Int. Conf. Robotics and Automation*, 2015.

[23] A. Myronenko and X. Song, "Point set registration: Coherent point drift," *IEEE Tran. on Pattern Analysis and Machine Intelligence*, 2010.

[24] F. Nageotte, C. Doignon, M. de Mathelin, P. Zanne, and L. Soler, "Circular needle and needle-holder localization for computer-aided suturing in laparoscopic surgery," pp. 87–98.

[25] S. Niekum, S. Osentoski, G. Konidaris, S. Chitta, B. Marthi, and A. G. Barto, "Learning Grounded Finite-State Representations from Unstructured Demonstrations," *Int. J. of Robotics Research*, 2015.

[26] C. C. L. or Open Resection Study Group *et al.*, "Laparoscopic surgery versus open surgery for colon cancer: short-term outcomes of a randomised trial," *The lancet oncology*, 2005.

[27] N. Padoy and G. Hager, "Human-Machine Collaborative Surgery using Learned Models," in *Proc. IEEE Int. Conf. Robotics and Automation (ICRA)*, 2011, pp. 5285–5292.

[28] S. Patil, Y. Duan, J. Schulman, K. Goldberg, and P. Abbeel, "Gaussian belief space planning with discontinuities in sensing domains," in *Proc. IEEE Int. Conf. Robotics and Automation (ICRA)*, 2014.

[29] S. Qureshi, K. Rupp, and B. Thompson, "Needle holder with suture filament grasping abilities," Sept. 14 1999, uS Patent 5,951,587.

[30] C. E. Reiley and G. D. Hager, "Task versus Subtask Surgical Skill Evaluation of Robotic Minimally Invasive Surgery," in *Medical Image Computing and Computer-Assisted Intervention (MICCAI)*, 2009.

[31] J. Schulman, Y. Duan, J. Ho, A. Lee, I. Awwal, H. Bradlow, J. Pan, S. Patil, K. Goldberg, and P. Abbeel, "Motion planning with sequential convex optimization and convex collision checking," *The International Journal of Robotics Research*, 2014.

[32] J. Schulman, A. Gupta, S. Venkatesan, M. Tayson-Frederick, and P. Abbeel, "A case study of trajectory transfer through non-rigid registration for a simplified suturing scenario," 2013.

[33] J. Schulman, J. Ho, A. Lee, H. Bradlow, I. Awwal, and P. Abbeel, "Finding Locally Optimal, Collision-Free Trajectories with Sequential Convex Optimization," in *Robotics: Science and Systems (RSS)*, 2013.

[34] S. Speidel, A. Kroehnert, S. Bodenstedt, H. Kenngott, B. Mueller-Stich, and R. Dillmann, "Image-based tracking of the suturing needle during laparoscopic interventions," in *SPIE Medical Imaging*, 2015.

[35] C. Staub, T. Osa, A. Knoll, and R. Bauernschmitt, "Automation of tissue piercing using circular needles and vision guidance for computer aided laparoscopic surgery," in *Robotics and Automation (ICRA), 2010 IEEE International Conference on*, 2010.

[36] A. P. Stegemann, K. Ahmed, J. R. Syed, S. Rehman, K. Ghani, R. Autorino, M. Sharif, A. Rao, Y. Shi, G. E. Wilding, *et al.*, "Fundamental skills of robotic surgery: a multi-institutional randomized controlled trial for validation of a simulation-based curriculum," *Urology*, 2013.

[37] J. van den Berg, S. Miller, D. Duckworth, H. Hu, A. Wan, X.-Y. Fu, K. Goldberg, and P. Abbeel, "Superhuman performance of surgical tasks by robots using iterative learning from human-guided demonstrations," *Robotics and Automation (ICRA), 2011 IEEE International Conference on*, 2010.